

MODELING OF HVOF THERMAL SPRAY DEPOSITION OF NITINOL COATING: EFFECT OF SPRAYING PROCESS PARAMETERS ON GAS AND PARTICLES PROPERTIES AND COATING QUALITY

Carmen DE CRESCENZO ¹, Despina KARATZA ¹, Simeone CHIANESE ¹,
Konstantinos G.DASSIOS ², Dimitrios A.EXARCHOS ², Theodore E.MATIKAS ²,
Dino MUSMARRA ¹

¹Department of Engineering, University of Campania "Luigi Vanvitelli", Via Roma 29, Aversa (CE), Italy, EU
carmen.decrescenzo@unicampania.it; karatza@irc.cnr.it; simeone.chianese@unicampania.it;
dino.musmarra@unicampania.it

²Department of Materials Science and Engineering, University of Ioannina, 45110 Ioannina, Greece, EU
kdassios@cc.uoi.gr; dexarch@cc.uoi.gr; matikas@cc.uoi.gr

Abstract

In this work, modelling of Nitinol (Ni-45 wt.%Ti) coating deposition, by means of High Velocity Oxygen-Fuel (HVOF) technology, is presented. Species transport model and the $k-\epsilon$ turbulence model were solved in Ansys Fluent environment, in which combustion between kerosene and oxygen, gas and particle flow in a GTV HVOF-K2 gun (GTV Verschleiss-Schutz GmbH, Germany) were simulated. The effect of spraying process parameters, such as spray distance, particle shape factor, and kerosene to oxygen feed rate ratio, affecting coating properties and quality, on the supersonic gas flow dynamics, particle velocity and temperature, was numerically investigated. Moreover, correlation between modelling findings and coating quality was explored. Numerical findings highlighted that the higher the kerosene to oxygen feed rate ratio the higher the temperatures and velocities of both gas and particles and the combustion pressure; moreover, with particle shape factor lower than 1, velocity of particles increased while ultimate temperature decreased. Furthermore, the findings of this study allowed to predict the properties of impacting Nitinol particles on substrates and showed the thermal story of the particle from the injection to the impact. These above-mentioned aspects are of great importance because Nitinol is a Shape Memory Alloy and its performances strongly depend on stress and thermal state.

Keywords: Nitinol, HVOF, numerical simulations, CFD, gas flow dynamics, particle properties

1. INTRODUCTION

Thermal spray High Velocity Oxygen-Fuel (HVOF) is a particulate deposition process which allows to produce homogeneous [1] and very dense coatings [2,3] with low oxide content [1,4], high hardness [2,5], and excellent bond strength [1,2,5]. Particles of metals, alloys, or cermets, are injected in a hot gaseous stream produced by the combustion of oxygen and gaseous or liquid fuels, and are propelled at supersonic or hypersonic velocities [5,6] towards the substrate to be coated. The properties of a thermally sprayed coating are strongly linked to particle velocity, temperature and in-flight behaviour, which in turn depend on spraying and coating process parameters, such as spray distance [7,8], fuel to Oxygen ratio [5,9], powder feed rate [7,10] and particle size [8,11]. The evolution of gas and particle temperature and velocity and the influence of process variables on particle properties in gas and liquid-fuelled systems were investigated in several papers [5,8,10,11]. In the present work, Nitinol (Ni-45 wt.%Ti) coating deposition by a GTV HVOF-K2 gun thermal spray (GTV Verschleiss-Schutz GmbH, Germany) was simulated in 2D, using the computational fluid dynamics software Ansys Fluent, in which species transport model, $k-\epsilon$ turbulence model and discrete phase model

(DPM) were implemented. The CFD simulation was performed to define the effect of standoff distance, fuel to oxygen feed rate ratio and particle shape factor on velocity and temperature of Nitinol particles, in order to investigate the thermal story of the Nitinol particle from the injection to the impact. The gas flow characteristics such as temperature, pressure and velocity were also investigated.

Nomenclature

A_p , surface area of the particle	Re , Reynolds number	<i>Greek letters</i>
C_D , drag coefficient	R_α , species net production rate	μ , viscosity
c_p , specific heat of the particle	S_α , generating rate	μ_t , turbulent viscosity
d_p , particle diameter	S_h , chemical reaction source energy	ρ , density
E , enthalpy	T , temperature	τ , deviatoric stress tensor
F_x , additional acceleration	T_g , gas temperature	φ , equivalence ratio
H , heat transfer coefficient	T_p , particle temperature	
J_α , mass diffusion flux	u , velocity	<i>Subscripts</i>
K , thermal conductivity	u_i , velocity in the i-direction	α , species
k_{eff} , effective thermal conductivity	u_p , particle velocity	g , gas
m_p , mass of the particle	x_i , coordinate in the i direction	i, j , coordinate indices
p , pressure	Y_α , mass fraction of each species	p , particle

2. MATHEMATICAL MODELS

The 2D schematic diagram of the GTV HVOF-K2 gun is sketched in **Figure 1**, in which fuel (kerosene) and oxygen inlet, combustion chamber, convergent-divergent (CD) nozzle, Nitinol injection, barrel, external domain, and boundary conditions adopted in the simulations are illustrated.

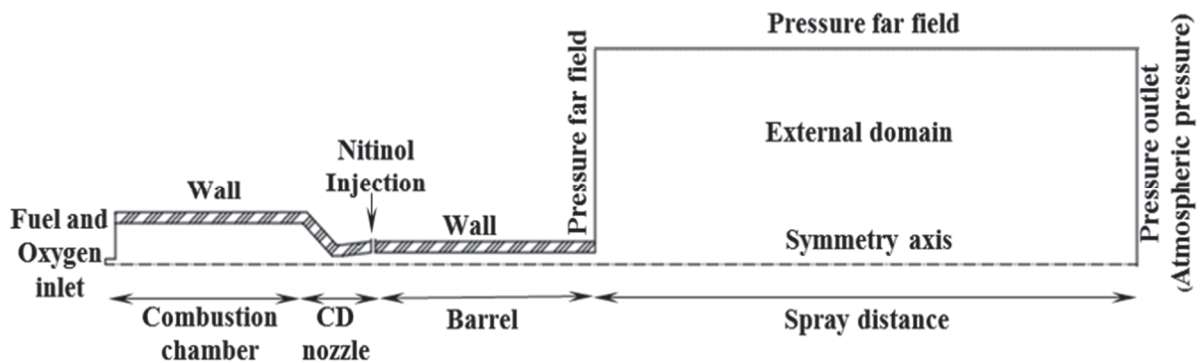


Figure 1 Schematic diagram of GTV HVOF-K2 gun and boundary conditions adopted in the simulations

The length in axial direction of the combustion chamber, the CD nozzle and the barrel are 92.5 mm, 33.0 mm and 111.1 mm, respectively. Kerosene and oxygen streams are fed in the combustion chamber, burn and combustion products are accelerated along the CD nozzle and barrel. Nitinol powder particles are injected at the end of the combustion chamber and are propelled by combustion gases towards the substrate to be coated. The CFD model was implemented in Ansys Fluent 14.5 environment and simulations were performed by means of finite element approach. An axisymmetric geometry and a two-dimensional model were employed to reduce the complexity and computational time. A structured grid was built in the whole domain and meshes were refined in the nozzle entrance and exit, the barrel exit and the free-jet centreline, in order to define more accurately flame flow and particle properties in the more sensitive sections of the gun.

2.1. Gas flow dynamics

A “realizable k - ε model” was used for modelling gas flow in HVOF simulations. The governing equations for the 2D model in the Cartesian tensor form [12] are:

- Mass conservation equation:

$$\frac{\partial \rho}{\partial t} + \frac{\partial}{\partial x_i} (\rho u_i) = 0 \quad (1)$$

- Momentum conservation:

$$\frac{\partial}{\partial t} (\rho u_i) + \frac{\partial}{\partial x_j} (\rho u_i u_j) = - \frac{\partial \rho}{\partial x_i} + \frac{\partial}{\partial x_j} (\tau_{ij})_{eff} + \frac{\partial}{\partial x_j} (-\overline{\rho u_i u_j}) \quad (2)$$

- Energy transport equation:

$$\frac{\partial}{\partial t} (\rho E) + \frac{\partial}{\partial x_i} [u_i (\rho E + \rho)] = \frac{\partial}{\partial x_j} (k_{eff} \frac{\partial T}{\partial x_j} + u_i (\tau_{ij})_{eff}) + S_h \quad (3)$$

2.2. Species transport

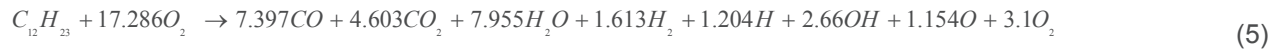
The volumetric combustion reaction was simulated using a Species Transport model with an Eddy-Dissipation turbulence-chemistry interaction.

$$\frac{\partial}{\partial x_i} (\rho Y_\alpha u_i) = - \frac{\partial J_{\alpha,i}}{\partial x_i} + R_\alpha + S_\alpha \quad \alpha = 1, 2, \dots, N \quad (4)$$

where N is the total number of fluid phase chemical species present in the system [13].

2.3. Combustion model

Liquid kerosene (C₁₂H₂₃) combustion is a very complex mechanism and consist of hundreds of species and irreversible and reversible reactions [11]. In this work, the chemical reaction was assumed as a single-step reaction, including only CO₂, CO, H₂O, H₂, OH, H, O₂ and O as products, and is reported below [14]:



2.4. Particle model

The gas phase as continuum was solved by using Navier-Stokes equations. The liquid phase was introduced as large number of droplets in the gun which trajectories, heat and mass transfer with gas phase were computed using Discrete Phase Model (DPM). The particle motion in the x direction in Cartesian coordinates can be solved by the force balance that equates the droplet inertia with forces acting on the particle. The particle motion can be described by the following equation [5,15]:

$$\frac{\partial u_p}{\partial t} = \frac{18\mu}{\rho_p d_p^2} \frac{C_D Re}{24} (u - u_p) + F_x \quad (6)$$

The energy equation for a single particle, neglecting the heat transfer through radiation, can be written as it follows [16]:

$$m_p c_p \frac{dT_p}{dt} = hA_p (T_g - T_p) \quad (7)$$

3. RESULTS AND DISCUSSION

3.1. Effect of kerosene and oxygen feed rate ratio

The effect of kerosene-oxygen equivalence ratio ($\phi = 0.75; 0.77; 0.83$) on gas temperature, gas pressure and gas axial velocity as function of the axial distance, along the symmetry line, was investigated by using a standoff distance of 300 mm and a particle shape factor (SF) of 1. Kerosene and oxygen were injected into the combustion chamber at the mass flow inlet boundary condition. Results are reported in **Figure 2**.

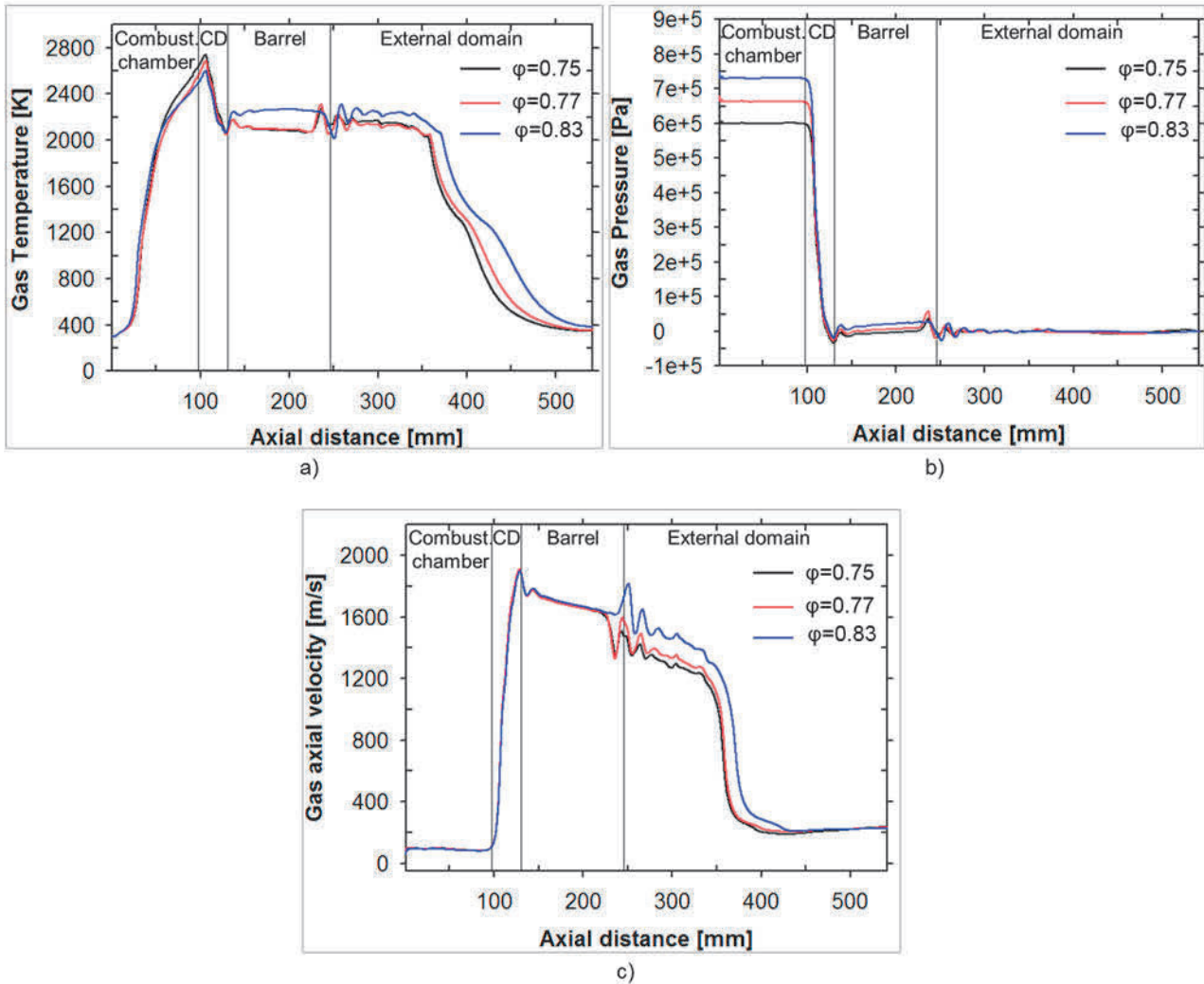


Figure 2 Effect of equivalence ratio on a) gas temperature, b) gas pressure and c) gas axial velocity

Gas temperature trends show peaks in the CD nozzle, after which drastically decrease till to stable values, followed by a fast reduction. Peaks seem not to be particularly affected by the equivalence ratio, while at the outlet of the combustion chamber the highest values for $\phi = 0.83$ can be seen. Gas pressure trends show the highest values in the combustion chamber, rapid decreasing up to values below atmospheric pressure and fluctuations caused by over-expanding and then re-converging both above and below atmospheric pressure. Maximum relative pressures of 6.4×10^5 Pa, 7.1×10^5 Pa, and 7.8×10^5 Pa, for $\phi = 0.75$, $\phi = 0.77$, and $\phi = 0.83$, are respectively reported, in agreement with the values measured during nitinol coating deposition experimental activity at the same operating conditions. Gas velocity trends show the lowest values in the combustion chamber, at which it follows a rapid increase in the convergent part of nozzle for a successive slow reduction in the divergent one. The higher the equivalence ratio the higher the gas velocity. Nitinol particles,

with a size range of 15-45 μm and a Rosin-Rammler diameter distribution, are injected with a mass rate of 70 g/min. **Figure 3** depicts Nitinol particle temperature and velocity for an average particle diameter of 30 μm : the higher the equivalence ratio the higher the temperature and the velocity of particles.

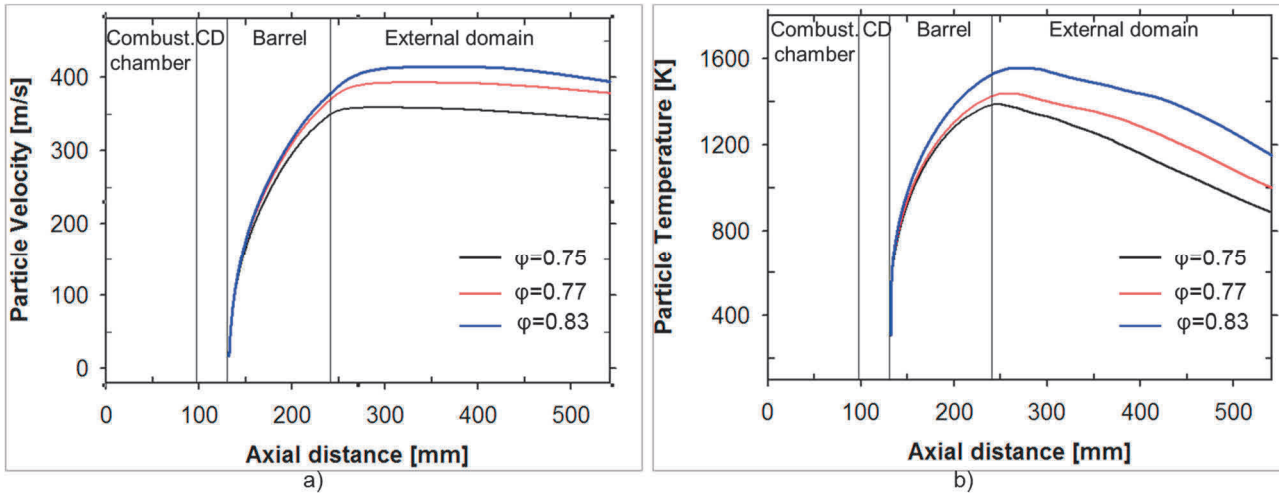


Figure 3 Effect of equivalence ratio on average diameter 30 μm particle a) temperature and b) axial velocity

3.2. Effect of particle shape factor

The effect of particle shape factor (SF) on particle temperature and velocity in the range 0.7-1 was investigated. Shape factor is used for defining the degree sphericity and represents the ratio of the actual surface area of the non-spherical particle to the surface area of the sphere of the same volume as the non-spherical particle. Simulations were performed by using a standoff distance of 300 mm, an equivalence ratio of 0.75 and an average particle diameter of 30 μm . Results are shown in **Figure 4**. As it can be seen, the lower the shape factor the higher the particle velocity, because of the axial gas flow exerts a drag force larger on non-spherical particles ($\text{SF} < 1$) than spherical ones ($\text{SF} = 1$) [17]. Particle temperature in the barrel decreases with decreasing of SF because of the higher velocities that imply shorter residence time in the flame.

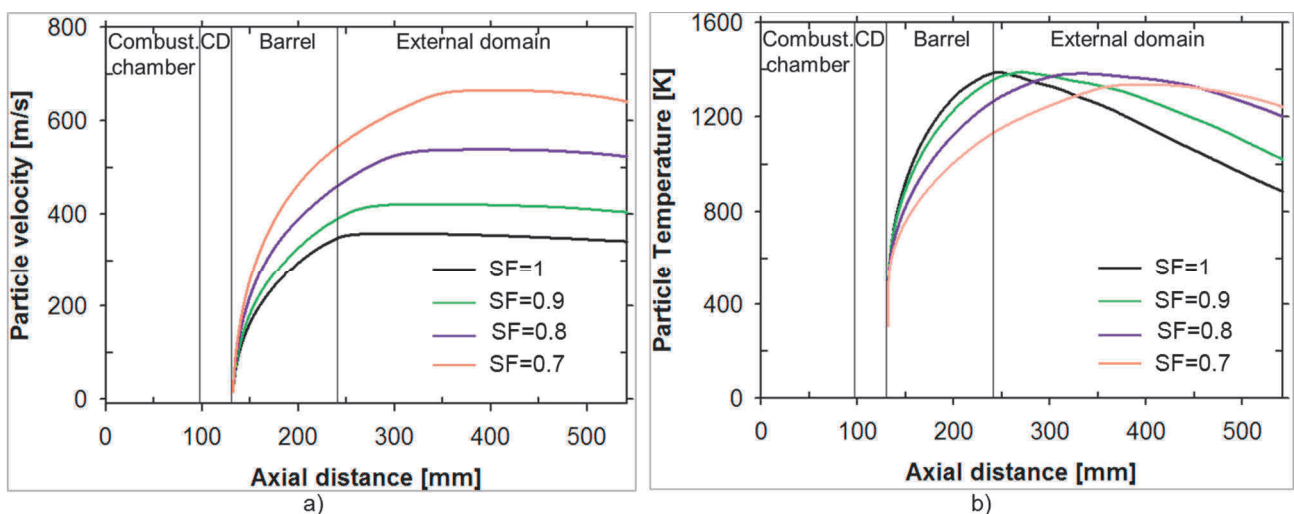


Figure 4 Effect of particle shape factor on a) particle temperature and b) axial velocity

3.3. Effect of spray distance

HVOF Thermal Spray was simulated with variable standoff spray distance of 300 mm, 350 mm and 400 mm, in order to define particle properties at impact on the substrate. Simulations were carried out by using $\phi=0.75$ and $SF=1$. As can be seen in **Figure 5**, impact particle temperature decreases from a maximum of 886 K at a standoff distance of 300 mm to a minimum of 723 K at 400 mm. Accordingly, particle velocity at impact decreases from a maximum value of 342 m/s at a standoff distance of 300 mm to a minimum of 322 m/s at 400 mm. The optimal spray distance value reasonably is identified in 300 mm because the higher velocities ensure higher impact energy and greater adhesion. The particles temperatures found are below Nitinol melting temperature, hence Nitinol particles impacting on substrates are in solid state.

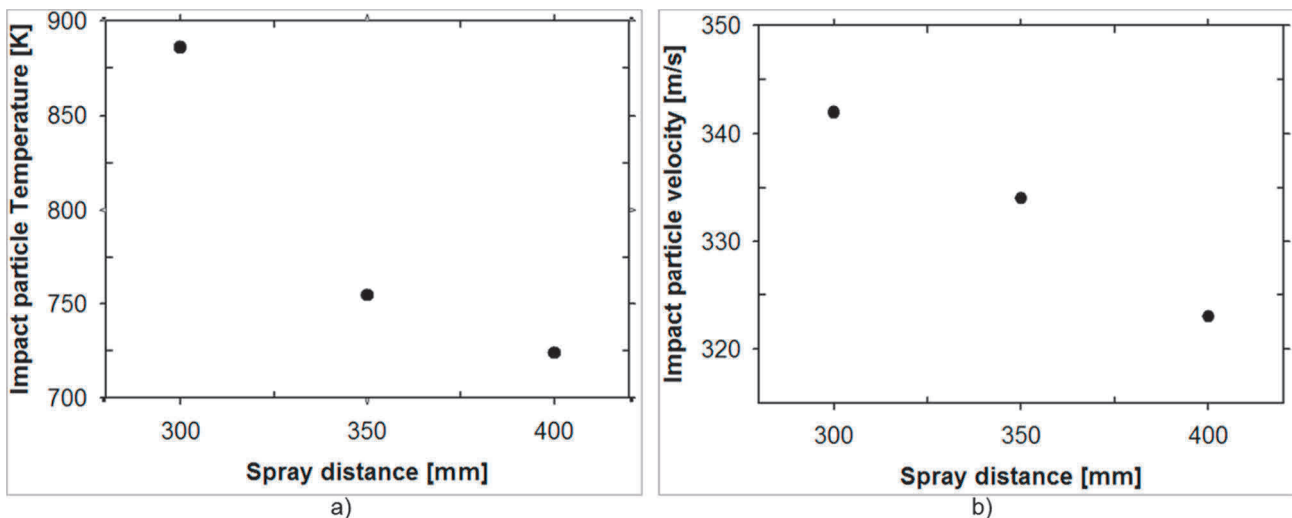


Figure 5 Particle temperature and velocity at impact at different standoff distance

4. CONCLUSIONS

This work presents results of simulations of a HVOF coating deposition. The model was developed in Ansys Fluent environment and flame and Nitinol particle behaviour were investigated. As shown, the higher the values of ϕ the higher the values of gas temperature, pressure and velocity; while Nitinol particles reach higher velocities and temperatures with $\phi=0.83$. Particle velocity decreases with increasing of SF from 0.7 to 1. As consequence, particle temperature in the barrel increases with SF . Furthermore, influence of standoff distance on Nitinol particles velocity and temperature at impact was investigated, finding that both decrease with increasing of spray distance.

ACKNOWLEDGEMENT

This manuscript has been financially supported under "Horizon 2020 - The Framework Programme for Research and Innovation (2014-2020): Future and Emerging Technologies (FET Open)", project title: "An Innovative Method for Improving the Structural Integrity using SMA Revolutionary Technology (InnoSMART)" - Grant Agreement No 664892.

REFERENCES

- [1] RUIZ-LUNA, H., LOZANO-MANDUJANO, D., ALVARADO-OROZCO, J.M., VALAREZO, A., POBLANO-SALAS, C.A., TRÁPAGA-MARTÍNEZ, L.G., ESPINOZA-BELTRÁN, F.J. and MUÑOZ-SALDAÑA, J. Effect of HVOF processing parameters on the properties of NiCoCrAlY coatings by design of experiments. *J. Therm. Spray Techno.* 2014. vol. 23, iss. 6, pp. 950-961.

- [2] SIDHU, T.S., PRAKASH, S. and AGRAWAL, R.D. Studies on the properties of high-velocity oxy-fuel thermal spray coatings for higher temperature applications. *Mater. Sci.* 2005. vol. 41, iss. 6, pp. 805-823.
- [3] XIE, M., LIN, Y., KE, P., WANG, S., ZHANG, S., ZHEN, Z. and GE, L. Influence of Process Parameters on High Velocity Oxy-Fuel Sprayed Cr₃C₂-25%NiCr Coatings. *Coatings*. 2017. vol. 7, iss. 7, art. no. 98.
- [4] TOTEMEIER, T.C., WRIGHT, R.N. and SWANK, W.D. FeAl and Mo-Si-B intermetallic coatings prepared by thermal spraying. *Intermetallics*. 2004. vol. 12, iss. 12, pp. 1335-1344.
- [5] TABBARA, H., GU, S. Computational simulation of liquid-fuelled HVOF thermal spraying. *Surf. Coatings Technol.* 2009. vol. 204, iss. 5, pp. 676-684.
- [6] WANG, X., SONG, Q. and YU, Z. Numerical Investigation of Combustion and Flow Dynamics in a High Velocity Oxygen-Fuel Thermal Spray Gun. *J. Therm. Spray Technol.* 2016. vol. 25, iss. 3, pp. 441-450.
- [7] MARANHO, O., RODRIGUES, D., BOCCALINI, M. and SINATORA, A. Influence of parameters of the HVOF thermal spray process on the properties of multicomponent white cast iron coatings. *Surf. Coatings Technol.* 2008. vol. 202, iss. 15, pp. 3 494-3500.
- [8] GU, S., EASTWICK, C.N., SIMMONS, K.A. and MCCARTNEY, D.G. Computational Fluid Dynamic Modelling of Gas Flow Characteristics in a High-Velocity Oxy-Fuel Thermal Spray System. *J. Therm. Spray Technol.* 2001. vol. 10, iss. 3, pp. 461-469.
- [9] SAEEDI, B. and ROUHAGHDAM, A.S. The study of high temperature oxidation behavior of different microstructures of HVOF thermally sprayed coatings. *J. Adv. Mater. Process.* 2014. vol. 2, iss. 2, pp. 3-11.
- [10] WANG, Y., JIANG, S.L., ZHENG, Y.G., KE, W., SUN, W.H., CHANG, X.C., HOU, W. L. and WANG, J.Q., Effect of processing parameters on the microstructures and corrosion behaviour of high-velocity oxy-fuel (HVOF) sprayed Fe-based amorphous metallic coatings. *Mater. Corros.* 2013. vol. 64, iss. 9, pp. 801-810.
- [11] PAN, J., HU, S., YANG, L., DING, K. and MA, B. Numerical analysis of flame and particle behavior in an HVOF thermal spray process. *Mater. Des.* 2016. vol. 96, pp. 370-376.
- [12] KAMNIS, S. and GU, S. Numerical modelling of propane combustion in a high velocity oxygen-fuel thermal spray gun. *Chem. Eng. Process. Process Intensif.* 2006. vol. 45, iss. 4, pp. 246-253.
- [13] FLUENT INC. Ansys Fluent 14.5 User's Guide. 2011.
- [14] KUNDU, K., PENKO, P. and YANG, S. Reduced Reaction Mechanisms for Numerical Calculations in Combustion of Hydrocarbon Fuels. In: *36th AIAA Aerospace Sciences Meeting and Exhibit*. Reno, NV,U.S.A., 1998.
- [15] ZEOLI, N., GU, S. and KAMNIS, S. Numerical simulation of in-flight particle oxidation during thermal spraying. *Comput. Chem. Eng.* 2008. vol. 32, iss. 7, pp. 1661-1168.
- [16] KHAN, M.N. and TARIQ, S. Investigation of a dual-stage high velocity oxygen fuel thermal spray system. *Appl. Energy*. 2014. vol. 130, pp. 853-862.
- [17] HAIDER, A. and LEVENSPIEL, O. Drag coefficient and terminal velocity of spherical and nonspherical particles. *Powder Technol.* 1989. vol. 58, iss. 1, pp. 63-70.